Journal of Cleaner Production 229 (2019) 886–901

Contents lists available at ScienceDirect

Journal of Cleaner Production

journal homepage: www.elsevier.com/locate/jclepro

Life cycle burden-shifting in energy systems designed to minimize greenhouse gas emissions: Novel analytical method and application to the United States

Ibrahim M. Algunaibet [a], Gonzalo Guillén-Gosálbez [b, *]

[a] Centre for Process Systems Engineering, Department of Chemical Engineering, Imperial College London, South Kensington Campus, London, SW7 2AZ, UK
[b] Institute for Chemical and Bioengineering, Department of Chemistry and Applied Biosciences, ETH Zürich, Vladimir-Prelog-Weg 1, 8093, Zürich, Switzerland

ARTICLE INFO

Article history:
Received 3 January 2019
Received in revised form
22 March 2019
Accepted 22 April 2019
Available online 23 April 2019

Keywords:
Climate change
Elasticity
Energy systems modeling
IPAT
Life cycle assessment
STIRPAT

ABSTRACT

Energy systems are currently designed focusing only on minimizing their cost or, at most, including limits on greenhouse gas emissions. Unfortunately, electricity technologies performing well in global warming potential might not necessarily behave equally well across other sustainability criteria. Hence, policies focused solely on mitigating greenhouse gas emissions could potentially resolve one problem (i.e., climate change) by creating another, thereby leading to burden-shifting. Here, the occurrence and severity of burden-shifting in energy systems design are both investigated through the application of a novel approach integrating multi-objective optimization, life cycle assessment and multivariate regression based on elasticities. Environmental impacts are classified into three categories: no burden-shifting, total burden-shifting and partial burden-shifting, providing for the latter two a measure of their severity. Due to inherent trade-offs in the life cycle performance of technologies, discussed in detail in this work, the Paris Agreement 2 °C targets would lead to burden-shifting in the United States (total or partial) in up to eight environmental impacts. On the other hand, stringent carbon emissions reductions in line with the 1.5 °C targets can lead to burden-shifting in three environmental impacts. Indeed, in both cases undesirable increases in some damage categories of up to 1.64% for every percentage increase in cost can take place as a result of more stringent limits on greenhouse gas emissions compared to the least cost solution. Overall, this work aims to foster fruitful discussions on how to generate energy within the Earth's ecological capacity by expanding the analysis beyond climate change.

© 2019 Elsevier Ltd. All rights reserved.

1. Introduction

Reducing Greenhouse Gas (GHG) emissions is a major concern worldwide, with initiatives such as the Paris Agreement seeking to keep the global average temperature below 1.5 to 2 °C above pre-industrial levels (UNFCCC, 2015a). Given its high carbon intensity, the power sector is key for attaining this goal, more so in countries such as China and the United States (US) that are responsible for a large share of total carbon emissions (IEA, 2018). The intricacy of the power sector is remarkable, whereby different electricity technologies exist and a wide range of reliability constraints need to be considered for a proper design and operation of the system. Energy systems models were originally developed to handle this complexity by optimizing the Levelized Cost of Electricity (LCOE) considering engineering and reliability constraints. Examples of such energy systems models include MARKAL/TIMES (Loulou et al., 2004), NEMS (EIA, 2011) and SWITCH (Fripp, 2012), which broadly agree on the mathematical formulation while differing in the underlying assumptions and limitations.

In the last years, energy systems models, traditionally focused on minimizing total costs, were enlarged in scope to incorporate limits on GHG emissions in line with global environmental trends (Amorim et al., 2014; Choi et al., 2017). This was first done focusing on production-based GHG emissions, while more recently emissions over the whole life cycle were incorporated into the underlying mathematical models (McDowall et al., 2018; Pehl et al., 2017). Life Cycle Assessment (LCA) principles provide invaluable insights into electricity technologies, some of which may seemingly

* Corresponding author.
E-mail address: gonzalo.guillen.gosalbez@chem.ethz.ch (G. Guillén-Gosálbez).

https://doi.org/10.1016/j.jclepro.2019.04.276
0959-6526/© 2019 Elsevier Ltd. All rights reserved.

show low (or even zero) emissions on a production-based basis (i.e., direct emissions) despite emitting CO_2 over their entire life cycle. For instance, Photovoltaics (PV) and wind power technologies have no direct emissions, yet emit CO_2 during their production phase (Wernet et al., 2016); consequently, quantifying emissions on a life cycle basis is of utmost importance in any environmental assessment, as otherwise spurious conclusions might be drawn.

While global warming is receiving most of the attention, other environmental burdens do exist that play also a key role in preserving the Earth's ecological capacity (Algunaibet et al., 2019b). LCA can be used to quantify these burdens by converting hundreds of life cycle inventory entries, often hard to interpret at a first glance (e.g., emissions of particulate matter, nickel, nitrogen oxides, etc.), into a set of more meaningful midpoint and endpoint life cycle impacts (e.g., the ReCiPe 2008 framework (Goedkoop et al., 2009)) easier to analyze, particularly by policymakers (Algunaibet et al., 2019a). These impacts quantify the effect of specific environmental stressors on environmental categories beyond climate change, such as human health and ecosystem diversity (Organization, 1997).

The inclusion of life cycle midpoints and endpoints in energy systems models is still in its infancy and merit further attention. Previous seminal works in this field already identified inherent trade-offs between life cycle categories in energy systems design (Algunaibet et al., 2019a), which appear because certain technologies perform well in some environmental criteria and poor in others (García-Gusano et al., 2018; Rauner and Budzinski, 2017). As an example, when attempting to attain 80% carbon reductions by 2050, some energy models found that some life cycle impacts, such as freshwater ecotoxicity and abiotic depletion, could worsen (Garcia-Gusano et al., 2017). This phenomenon by which an environmental problem is mitigated by worsening another is known as burden-shifting; unfortunately, burden-shifting appears in many areas in science and engineering, including the design of energy systems (Limleamthong and Guillen-Gosalbez, 2017; Mendoza et al., 2019), making the environmental analysis and associated decision-making process quite challenging. Indeed, the occurrence of burden-shifting is a well-known fact, for example, in biofuels production (i.e., climate change *vs* land occupation) (Reinhard and Zah, 2009) and nuclear power (i.e., climate change *vs* radioactive emissions) (Suman, 2018), among others. Despite its importance and wide implications in sustainability, there is no systematic method to study and quantify the severity of burden-shifting in environmental studies, a research gap that we address here.

A statistical framework coupled with multi-objective optimization and LCA is here proposed to quantify the occurrence and severity of burden-shifting across life cycle impacts; this approach is applied to analyze the implications of imposing stringent targets based solely on GHG emissions in energy systems design. The developed framework aims to enlarge the scope of some current environmental policies with limited scope that, in an attempt to mitigate some environmental problems, can unintentionally create others. The proposed approach makes use of the elasticity concept (Mas-Colell et al., 1995), widespread in economics, to evaluate the responsiveness of each life cycle impact to the stringency of 100-year Global Warming Potential (GWP100) targets, using to this end Pareto solutions of a multi-objective model as input data. This approach allows classifying environmental impacts in three main categories, according to whether burden-shifting occurs (total or partial) or not at all.

This method is applied to analyze trade-offs between life cycle impacts in the US Intended Nationally Determined Contribution (INDC) governed by the Paris Agreement 2 °C targets, or more severely the 1.5 °C targets (UNFCCC, 2015b). To this end, an energy systems model for the US, known as Emissions Reduction Cooperation Model with Life Cycle Impact Assessment (ERCOM-LCIA) (Algunaibet et al., 2019a), was extended to include all the life cycle impacts covered in the ReCiPe 2008 framework (Goedkoop et al., 2009). Thereafter, the improved model was used to mimic the current policymakers' decision-making process in designing energy systems, where the LCOE is minimized for a given target on GWP100 in line with the 1.5 and 2 °C mitigation pathways. Finally, a statistical framework underpinned by the concept of elasticity, known as the Impact, Cost and Emissions (ICE) model, was developed to analyze these Pareto solutions and gain valuable understanding on the occurrence of burden-shifting and its implications.

The paper is organized as follows: Section 2 describes the problem statement, Section 3 presents the methodology, Section 4 illustrates the case study, Section 5 shows the motivating example, Section 6 presents the results and discussions, while Section 7 draws the main conclusions of the work.

2. Problem statement

The design of energy systems with targets imposed only on GHG emissions is the primary focus of this work. Given a specific electricity demand, cost and emissions data and a set of engineering constraints and life cycle impacts for every electricity technology and state, the goal of the analysis is to assess the occurrence and severity of burden-shifting across life cycle impacts when the mix is designed considering only the LCOE and GWP100. Decisions to be made in the design of the mix include the type and capacities of technologies selected and their location across the US. In addition, we highlight the drawbacks of current environmental policies focusing solely on GWP100, such as the Paris Agreement, by developing a statistical framework underpinned by the concept of elasticities. The developed modeling framework to tackle the stated problem is described in the next section.

3. Methodology

The proposed approach for analyzing burden-shifting is made of three different ingredients: a multi-objective optimization-based energy systems model, a life cycle impact assessment analysis embedded in this mathematical model and the use of elasticities computed using the outcome of the multi-objective optimization model (Fig. 1). These three components of the proposed approach are described in detail next.

3.1. Energy systems model: the emissions reduction cooperation model with life cycle impact assessment

To demonstrate the proposed modeling framework, an energy systems model for the US called ERCOM-LCIA (Algunaibet et al., 2019a) is improved to include a set of life cycle impacts. ERCOM-LCIA minimizes the LCOE subject to meeting engineering and reliability constraints (e.g., generation potential), which are defined for every technology and state. ERCOM-LCIA is solved by assuming a fully cooperative strategy among states by which they cooperate to reduce emissions more efficiently. Data corresponding to ERCOM-LCIA can be found in previous publications (Algunaibet et al., 2019a; Galan-Martin et al., 2018). Additional data sources that quantify the life cycle performance of every electricity technology and state are given in the next subsection.

The scope of ERCOM-LCIA was expanded to include life cycle midpoint and endpoint impacts to ultimately assess the occurrence and severity of burden-shifting. The aim is to design the most cost-effective mix for an increasingly stringent target on GWP100 by solving ERCOM-LCIA 1,000 times, each corresponding to a different target (where targets are equally spread between a lower and an

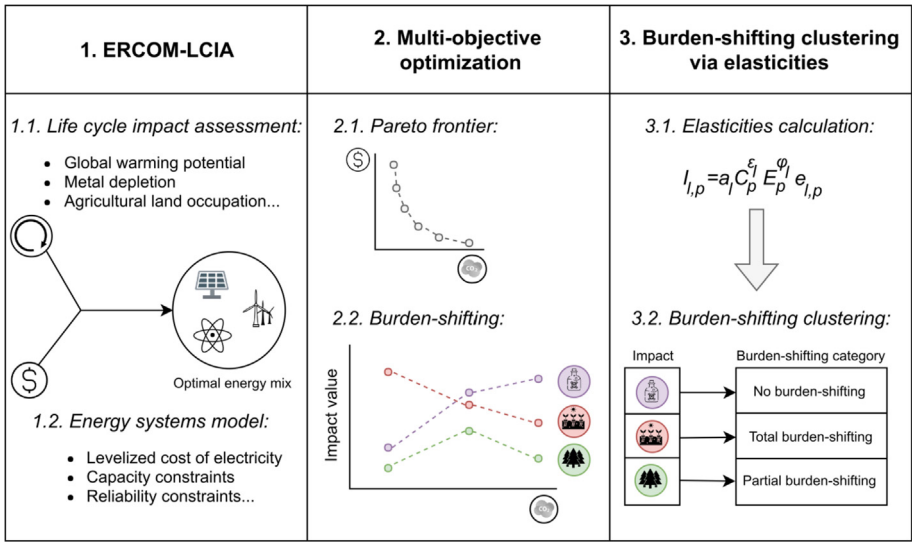

Fig. 1. Modeling framework for burden-shifting detection and categorization.

upper bound in line with the epsilon-constraint method (Murillo-Alvarado et al., 2015)); this mimics current policies that focus only on limiting GHG emissions. At each run, the least cost solution is found by solving an optimization model, which is recalculated by varying the limit on GWP100 from its lowest level to its highest one. The model can be described in compact form as follows (Appendices A and B show the full list of equality and inequality constraints that describe ERCOM-LCIA):

$$\min_{x,I}\left(\sum_{i,j} c_{i,j}^{T} x_{i,j}\right) \tag{1}$$

s.t.

$$\sum_{i,j} GWP100_{i,j} x_{i,j} \leq TARG \tag{2}$$

$$I_l = \sum_{i,j} CF_{i,j,l} x_{i,j} \qquad \forall l \tag{3}$$

$$B_{i,j} x_{i,j} \leq b_{i,j} \qquad \forall i,\ j \tag{4}$$

$$x, I \in \mathbb{R} \tag{5}$$

where $c_{i,j}^{T}$ is the LCOE for each electricity technology i and state j, $x_{i,j}$ is the electricity supplied by technology i and state j, $GWP100_{i,j}$ is the life cycle 100-year global warming potential per each unit of electricity supplied by technology i and state j, $TARG$ is the upper bound on the total GWP100, which is varied in each run, I_l is the total value for each life cycle impact l, $CF_{i,j,l}$ is the characterization factor for each life cycle impact l linked to the electricity supplied by technology i and state j, $B_{i,j}$ is a matrix of engineering constraints defined on each electricity technology i and state j, $b_{i,j}$ is the accompanying upper bound vector for every engineering constraint on each electricity technology i and state j and $\mathbb{R}$ is the set of real numbers to which $x_{i,j}$ and I_l belong.

3.2. Life cycle assessment

LCA quantifies environmental burdens of products and services across their entire supply chains (ISO, 2006), i.e., from cradle to grave, following four steps: goal and scope, inventory assessment, impact assessment and interpretation, which are described in detail next.

3.2.1. Goal and scope

LCA is applied to quantify the total environmental footprint of supplying one kWh of electricity (i.e., the functional unit) to meet the US demand for electricity in 2030, considering all the upstream activities in the energy supply chain. Taking the biomass power plant as an example, the LCA analysis here performed covers the harvesting of bioenergy sources, transport to the plant, construction of the power plant and combustion phase associated with the desired functional unit. The ReCiPe 2008 framework was used to assess the environmental performance of each electricity technology (Goedkoop et al., 2009), which translates thousands of life cycle inventory entries (e.g., CO_2 and forest transformation) into eighteen midpoint and three endpoint life cycle impacts.

3.2.2. Inventory assessment

In this step, the characterized inputs (e.g., raw materials) and outputs (e.g., emissions) required to generate one kWh of electricity are converted into environmental flows. These flows are categorized into three compartments, namely air, water and soil. The life cycle inventories for each electricity technology and state were retrieved from the ecoinvent database v3.4 (Wernet et al., 2016). Other technical sources were also used for those electricity technologies missing in the ecoinvent database, such as coal with Carbon Capture and Storage (CCS) (Iribarren et al., 2013), solar thermal (Corona et al., 2014) and natural gas with CCS (Petrakopoulou et al., 2015) power plants.

3.2.3. Life cycle impact assessment

To circumvent the complexity and nuances that would be introduced in a policymaking framework by the analysis of the many life cycle inventories, these were translated into a smaller set of more meaningful impacts via the ReCiPe 2008 framework (Goedkoop et al., 2009). These life cycle impacts include eighteen midpoints, summarized into three endpoints defined for human health, ecosystem diversity and resource availability, respectively. Overall, the eighteen midpoints can be classified into six clusters considering their environmental impact: (i) toxicity, (ii)

eutrophication, (iii) land-use, (iv) resource depletion, (v) emissions and (vi) acidification (Goedkoop et al., 2009).

Life cycle impacts within the toxicity cluster aim to measure the effect of chemicals accumulation in freshwater, terrestrial, human and marine compartments. Similarly, impacts belonging to the eutrophication cluster assess the nutrient enrichment in both fresh and marine waters. Land-use contains three impacts that quantify the damage to ecosystems as a result of the transformation of natural and urban lands alongside the occupation of agricultural lands. Depleting resources could also exert negative pressure on the sustainable development of future generations; hence, this cluster contains impacts such as water, fossil fuels and metals. Emissions also affect human health, in addition to climate change; hence, impacts within this cluster quantify GHG emissions related to global warming, particulate matter, photochemical oxidants, ozone depleting substances and ionizing radiation. Lastly, the only impact in the acidification cluster, namely the terrestrial acidification potential, measures the change in soil acidity due to the deposition of inorganic substances in the atmosphere that could potentially harm some species.

The aforementioned clusters of midpoints contribute differently to the three endpoint impacts: human health, ecosystem diversity and resource availability. For instance, human health is more strongly linked to GHG emissions, while land-use is connected to species diversity. Finally, resource availability is related to the depletion of finite fossil fuels and metals. Further details on the link between life cycle inventories, midpoints and endpoints can be found in the manual of the ReCiPe 2008 framework (Goedkoop et al., 2009).

In the analysis carried out in this work, burden-shifting across twenty of the twenty-one impacts is studied (i.e., eighteen midpoints and three endpoints) (Table 1); the GWP100 impact is, therefore, excluded from the burden-shifting assessment because it is employed as an explanatory variable instead of a dependent variable.

3.2.4. Interpretation of results

In this step, a comparison between conventional and new technologies is often carried out considering the calculated life cycle impacts. A handful of cases or scenarios are often designed to demonstrate the value of a given technology in pathways where they are needed the most. In this work, however, an alternative approach was taken. Following a previous work based on LCA and energy systems optimization (Rauner and Budzinski, 2017), the interpretation LCA phase is carried out by analyzing the Pareto frontier computed via ERCOM-LCIA, which contains a set of electricity mixes each achieving a unique combination of cost and LCA performance. This analysis is complemented with a statistical framework based on elasticities that evaluate the occurrence and severity of burden-shifting between life cycle impacts due to low, medium and high reduction targets on GWP100 in line with the 1.5 and 2 °C mitigation pathways. The statistical framework is described in the next subsection.

3.3. A statistical framework to characterize the occurrence and severity of burden-shifting: the ICE model

While no statistical framework was developed to assess burden-shifting, some attempted to address the responsiveness of an impact to given economic driving forces via elasticities – a concept wildly used in economics (Mas-Colell et al., 1995). Though the concept of elasticities is typically used to measure the demand responsiveness of a given commodity to its price and consumers' income levels (e.g., gasoline price elasticities (Algunaibet and Matar, 2018)), others attempted to adapt such concept to quantify the driving forces of environmental impacts. For instance, the IPAT (Ehrlich and Holdren, 1972) and ImPACT (Chertow, 2000) models proposed mathematical frameworks to quantify the extent to which a given environmental impact could vary due to changes in the population, affluence and technology assuming a proportional functional form (i.e., doubling the affluence results in doubling the impact when the other explanatory variables are held constant). Since such fixed proportionality assumption might not be applicable to all systems (Grossman and Krueger, 1995), others reformulated the IPAT and ImPACT models by allowing the explanatory variables to be raised to a power that does not necessarily equal one to consider non-proportional relationships, thereby leading to the STIRPAT model (York et al., 2003). Nonetheless, the STIRPAT model does not explicitly consider the technological driving force, as it often focuses on the population and affluence while attempting to infer the technological impact (York et al., 2003).

To explicitly consider the technological driving force, an extension of the STIRPAT model is proposed, referred to as the ICE model henceforth, to interpret the changes in life cycle impacts, I, via two driving forces typically used in designing energy systems and directly influenced by technologies, namely the cost of electricity, C, and emissions bound, E, as follows:

$$I_{l,p} = a_l C_p^{\varepsilon_l^c} E_p^{\varepsilon_l^e} e_{l,p} \tag{6}$$

where $I_{l,p}$ is the life cycle impact value for each impact l and Pareto point p, a_l is a coefficient that scales the multivariate model for each life cycle impact l, C_p is the total cost of electricity supply for each Pareto point p, ε_l^c is the cost elasticity of each life cycle impact l, E_p is the total life cycle value of GWP100 for each Pareto point p, ε_l^e is the GWP100 elasticity of each life cycle impact l and $e_{l,p}$ is the error term for life cycle impact l and Pareto point p. For simplicity, the multivariate model in Eq. (6) can be expressed in a linear form by

Table 1
Standard units of life cycle impacts (Goedkoop et al., 2009).

Impact	Standard unit	Impact	Standard unit
Terrestrial ecotoxicity potential	kg 1,4-DCB-Eq	Damage to ecosystem diversity	species.yr
Damage to resource availability[a]	USD_{2013}	Metal depletion potential	kg Fe-Eq
Marine ecotoxicity potential	kg 1,4-DCB-Eq	Ozone depletion potential	kg CFC-11-Eq
Particulate matter formation potential	kg PM_{10}-Eq	Fossil depletion potential	kg oil-Eq
Terrestrial acidification potential	kg SO_2-Eq	Ionizing radiation potential	kg U235-Eq
Damage to human health	DALYs	Urban land occupation potential	m^2a
Freshwater ecotoxicity potential	kg 1,4-DCB-Eq	Natural land transformation potential	m^2
Marine eutrophication potential	kg N-Eq	Water depletion potential	m^3
Human toxicity potential	kg 1,4-DCB-Eq	Photochemical oxidant formation potential	kg NMVOC
Freshwater eutrophication potential	kg P-Eq	Agricultural land occupation potential	m^2a

[a] The standard unit of the resource availability impact in the ReCiPe 2008 framework is USD_{2000}, however, it was converted to USD_{2013} to match the monetary unit of the cost of electricity employed in this paper (Statistics, 2018).

applying the natural logarithm transformation as shown in Eq. (7).

$$\ln\left(I_{l,p}\right) = \ln(a_l) + \varepsilon_l^c \cdot \ln(C_p) + \varepsilon_l^e \cdot \ln(E_p) + \ln\left(e_{l,p}\right) \quad (7)$$

Other functional forms could be used instead of the one shown in Eq. (6), e.g., adding quadratic terms; doing so, however, would make the simple, straightforward interpretation of the obtained elasticities more challenging (as shown in subsection 3.3.1). Adding complex polynomial terms in Eq. (6), for instance, requires the computation of the first partial derivative with respect to the explanatory variable of interest in logarithmic form, which is needed to maintain the elasticity meaning (York et al., 2003). Therefore, complex polynomial terms should be thought of only when the simple formulation, Eq. (6), fails to predict the dependent variable at hand precisely (i.e., impact). Furthermore, the population and affluence could be simply added to Eq. (6) to increase its accuracy. Here, without loss of generality, the focus is to better understand the technological driving force on the environmental impact of interest. Note that, for simplicity and without loss of generality, in this work both the population and affluence are fixed by taking a single year in the analysis (i.e., 2030); this allows us to better demonstrate the usefulness of the proposed ICE model.

3.3.1. Cost and emissions elasticities

Due to the employed functional form in Eq. (6), the interpretation of the cost and emissions (referred to here as GWP100) elasticities becomes straightforward. As a result of the functional form used in Eq. (6), the cost (ε_l^c) and GWP100 (ε_l^e) elasticities are the coefficients of the natural logarithm of the cost (C_p) and GWP100 (E_p) explanatory variables in Eq (7), i.e., no partial derivatives are required as opposed to other more complex functional forms. A given elasticity can be interpreted as the impact's percentage change due to a one-percent change in one of the explanatory variables while the other factors are kept constant (Mas-Colell et al., 1995).

Elasticities, i.e., the coefficients of the explanatory variables in the ICE model (Eq. (7)), can be further divided into ranges to formalize their interpretation. An elasticity that is greater than one infers that the impact changes at a higher pace than the driving force in its exact direction (e.g., cost or GWP100), thereby reflecting an *elastic relationship*. An elasticity equals to one indicates that the impact is proportional to the driving force, a relationship referred to as *unit elastic* – as assumed in the IPAT and ImPACT models. However, a positive elasticity that is less than one indicates that the impact changes at a slower pace than the driving force in its exact direction, what is known as an *inelastic relationship*. Similarly, a negative elasticity between zero and minus one indicates that the impact changes at a slower pace than the driving force but in its opposite direction, reflecting a *negative inelastic relationship (*or *negative inelasticity)*. An elasticity of minus one indicates an inverse proportional relationship with the driving force, known as *negative unit elasticity*. Lastly, an elasticity below minus one indicates that the impact changes at a higher pace than the driving force in its opposite direction referred to as a *negative elastic relationship*.

3.3.2. Categorizing burden-shifting via elasticities

Here, the cost and GWP100 elasticities calculated from the ICE model are used to quantify the occurrence and severity of burden-shifting for every life cycle impact. As two elasticities are computed (i.e., two driving forces act on each life cycle impact, namely the cost of electricity and GWP100), the following three general categories, summarized in Table 2, are identified.

In the context of the design problem addressed here, it is expected that the cost of electricity will increase with more stringent targets on GHG emissions due to the deployment of less polluting and more expensive renewable technologies. Therefore, when the sign of the cost elasticity is negative and the GWP100 elasticity is positive, no burden-shifting occurs since the life cycle impact will improve when GWP100 decreases (and the cost increases) due to more stringent targets on GWP100. When the sign of the cost elasticity is positive and the GWP100 elasticity is negative, however, total burden-shifting occurs since the life cycle impact will worsen when the GWP100 decreases (and the cost increases) due to stringent targets on GWP100. Lastly, the partial burden-shifting category depends on the target severity on GWP100. While it is best to compute elasticities with several data points, they can also be estimated between two different observations if needed. In the latter case, a perfect fit with a zero-approximation error would be obtained. Although the general categories reported in Table 2 remain valid in any application, the interpretation, meaning and implications of the elasticities' signs may differ depending on the relationship between the explanatory variables (e.g., cost and GWP100).

It is equally important to assess the coefficient of determination, R^2, before deriving conclusions from the multivariate model, Eq. (7). Indeed, a poor fit would yield elasticities that capture neither the occurrence nor the severity of burden-shifting. This would indicate that the life cycle impact at hand cannot be described by the explanatory variables (i.e., cost and GWP100). Hence, it is crucial to assess the coefficient of determination before drawing meaningful conclusions, as reported in Table 2.

4. Case study: energy systems

To demonstrate the capabilities of the proposed methodology, we apply it to data from the Pareto frontier of ERCOM-LCIA. Nevertheless, the proposed approach could be applied to any data set, not necessarily generated via mathematical models.

As described in subsection 3.1, ERCOM-LCIA mimics the current policymakers' approach towards the development of new regulations, based on identifying the least cost solution to meet varying targets on GWP100 while satisfying a given electricity demand. ERCOM-LCIA offers rich technological details, allowing the proposed ICE model to measure the technological driving force linked to environmental impacts. ERCOM-LCIA models thirteen electricity technologies: coal and natural gas with and without CCS, nuclear, hydropower, biomass, geothermal, PV rural and rooftop, wind onshore and offshore and solar thermal plants. For each technology, data on cost and twenty-one life cycle impacts were gathered, including the GWP100 taken as an explanatory variable in the ICE framework.

The upper bounds on GWP100 used to construct the Pareto frontier following the epsilon-constraint method are in line with the US INDC governed by the Paris Agreement 2 °C targets or, more severely, 1.5 °C targets (UNFCCC, 2015b). Thus, the aim of the study is to evaluate how the different life cycle impacts change when more stringent targets on GWP100 are imposed, to ultimately ascertain the extent to which burden-shifting (i.e., one impact improves at the expense of worsening others) occurs. To this end, once the Pareto points are at hand, the ICE model (Eq. (7)) is used to fit them, where the cost of electricity and GWP100 are the explanatory variables, while the dependent variables are the remaining twenty life cycle impacts (Fig. 2).

ERCOM-LCIA takes the form of a linear programming model that can be easily solved with state-of-the-art software packages and optimization solvers (e.g., CPLEX and GUROBI). The General Algebraic Modeling System (GAMS) (Brooke et al., 1998) version 25.0.2 was used to implement ERCOM-LCIA. For the case later described in detail, ERCOM-LCIA features 12,781 continuous variables and 8,921 constraints. ERCOM-LCIA was solved via the GUROBI solver version

Table 2
General categories of burden-shifting. GWP100 denotes the 100-year global warming potential.

Category type	Category description
No burden-shifting	No burden-shifting with any GWP100 target
Total burden-shifting	Impact worsens with any GWP100 target
Partial burden-shifting	Burden-shifting occurrence depends on the stringency of the GWP100 target

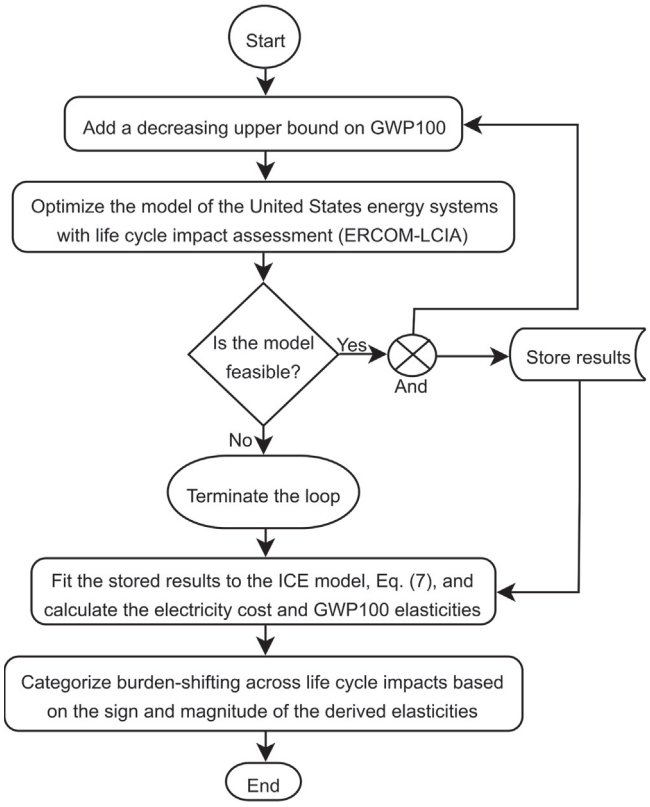
Start
Add a decreasing upper bound on GWP100
Optimize the model of the United States energy systems with life cycle impact assessment (ERCOM-LCIA)
Is the model feasible?
Yes
And
Store results
No
Terminate the loop
Fit the stored results to the ICE model, Eq. (7), and calculate the electricity cost and GWP100 elasticities
Categorize burden-shifting across life cycle impacts based on the sign and magnitude of the derived elasticities
End

Fig. 2. Flowchart diagram that demonstrates the steps taken to determine the occurrence and severity of burden-shifting across life cycle impacts. GWP100 stands for the 100-year global warming potential and ERCOM-LCIA denotes the Emissions Reduction Cooperation Model with Life Cycle Impact Assessment, i.e., the employed energy systems model in this work.

7.5.2 on an Intel®Core™ i7-6700 processor operating at 3.40 GHz, where each run consumes around 0.39 CPU seconds to close a zero-optimality gap.

5. Motivating example

Here, an example is presented to further motivate the need for the proposed statistical framework and clarify the concept of burden shifting. Note that the data contained in this motivating example (i.e., Section 5) were synthesized and do not correspond to any real scenario; this is done on purpose to illustrate more easily the aim and usefulness of the proposed framework in Section 3. Furthermore, the example has been set up without solving ERCOM-LCIA, focusing on three potential energy mixes with different environmental performance that could be found in practice.

5.1. The occurrence of burden-shifting

Suppose the cost of electricity needs to be minimized subject to meeting different levels of GWP100 targets (i.e., none, low and high). For each pair of explanatory variables, in this case GWP100 and cost of electricity, the performance of four additional sustainability criteria is studied, namely marine ecotoxicity, agricultural land occupation, metal depletion and natural land transformation potentials – again, the choice of these sustainability criteria is completely arbitrary and made to motivate the proposed framework. Fig. 3 shows the cost of electricity associated with each target on GWP100 (i.e., Pareto frontier) and the resultant performance in each sustainability criterion. Three main energy mixes are considered, each achieving a unique combination of cost and environmental impacts in line with the targets imposed; all depicted in Fig. 3. Clearly, the pattern of each sustainability criterion in Fig. 3, i.e., how each impact varies as more stringent targets on GWP100 are imposed, is hard to understand in the more general case, as it might be highly case dependent.

Taking a closer look at each sustainability criterion, it is found, for example, that marine ecotoxicity potential does not worsen with any target on GWP100; consequently, it does not show burden-shifting. On the other hand, agricultural land occupation potential worsens with any target on GWP100, that is, it does show burden-shifting. Metal depletion and natural land transformation potentials do not fully follow the pattern of GWP100. Focusing only on GWP100 while omitting other impacts could clearly induce burden-shifting between sustainability criteria, that is, one sustainability problem would be solved by creating another. This graphical analysis, easy to apply for the case of three solutions and three criteria, could become more challenging with an increasing number of mixes and environmental objectives. Furthermore, the graphical method as such does not quantify the severity (i.e., intensity) of burden shifting. Therefore, an approach that can systematically delineate each pattern of burden-shifting, including its occurrence and severity, is needed to investigate this phenomenon in a more systematic manner. In the next subsection, the proposed framework is applied to this motivating example.

5.2. Motivating example revisited: detecting and categorizing the occurrence of burden-shifting

To illustrate the usefulness of the framework proposed, the motivating example presented previously is next revisited. Recall that Fig. 3 shows the lowest cost for each target on GWP100 (i.e., Pareto frontier) along with the associated performance in marine ecotoxicity, agricultural land occupation, metal depletion and natural land transformation potentials. By applying the ICE model, Eq. (7), to the data in Fig. 3, the cost and GWP100 elasticities in Table 3 are obtained.

Instead of looking solely at the performance of every sustainability criterion in Fig. 3, the additional analysis in Table 3 systematically summarizes the occurrence and severity of each burden-shifting category. For example, marine ecotoxicity potential shows a negative cost elasticity and positive GWP100 elasticity and, hence, it does not worsen with any target on GWP100. In other words, marine ecotoxicity potential decreases when GWP100 declines due to the GWP100 positive elasticity and decreases when the cost increases due to the negative cost elasticity. Agricultural land occupation potential, however, worsens with any target on GWP100. Indeed, agricultural land occupation potential shows a

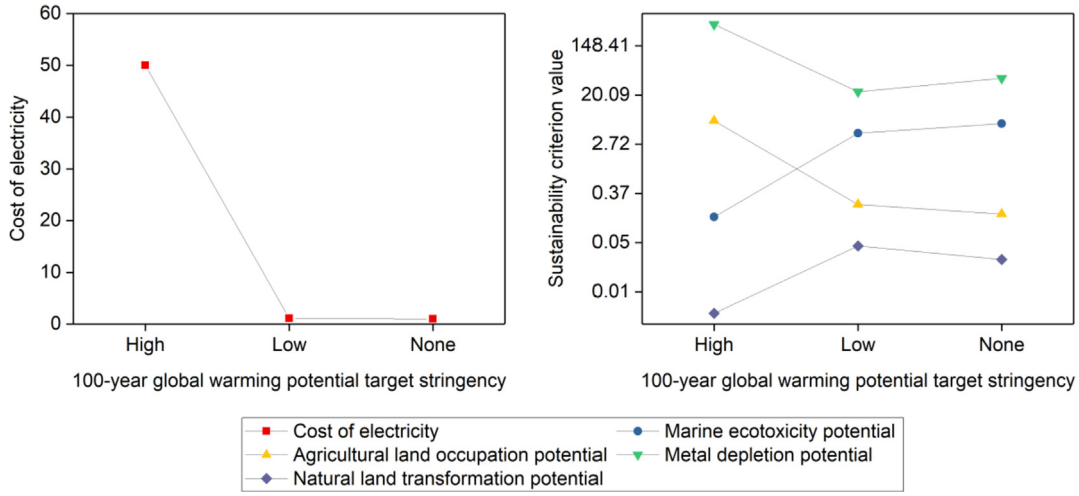

Fig. 3. Motivating example: An illustration of the concept of burden-shifting between sustainability criteria due to myopic environmental policies. Scatter plot on the left represents the Pareto frontier of the cost of electricity and 100-year global warming potential target stringency. Scatter plot on the right represents the resultant performance of each sustainability criterion due to different subjective targets on the 100-year global warming potential (i.e., none, low and high). Note the data underlying this figure were synthesized to illustrate the aim of the proposed framework.

Table 3
Cost of electricity and GWP100 elasticities for each sustainability criterion highlighted in the motivating example in Fig. 3. GWP100 denotes the 100-year global warming potential. Note the data for the analyzed sustainability criteria in Section 5 were designed to illustrate the aim of the proposed framework.

Impact	Cost elasticity	GWP100 elasticity
Marine ecotoxicity potential	−0.50	0.50
Agricultural land occupation potential	0.50	−0.50
Metal depletion potential	1.50	1.00
Natural land transformation potential	−1.50	−1.00

negative GWP100 elasticity and, hence, it increases when GWP100 decreases. Agricultural land occupation potential also increases when cost increases due to the positive cost elasticity. Finally, metal depletion and natural land transformation potentials follow a partial burden-shifting pattern, i.e., target-dependent burden-shifting. For instance, metal depletion potential decreases with low to medium GWP100 targets due to the positive GWP100 elasticity and increases when the cost increases due to the positive cost elasticity. On the other hand, natural land transformation potential behaves in an opposite manner compared to metal depletion potential. For example, natural land transformation potential increases with low to medium targets on GWP100 due to the negative GWP100 elasticity and decreases when the cost increases due to the negative cost elasticity.

It is equally important to pay attention to the magnitude of the elasticity, particularly, in instances where burden-shifting occurs. Elasticities that are greater than one, in absolute value, imply that the sustainability criterion at hand exhibits elastic responsiveness to the explanatory variable, as described in subsection 3.3.1. In the motivating example (Fig. 3), for instance, metal depletion potential has an elastic cost elasticity; therefore, one unit of percentage change in the cost – when all other factors are held constant – leads to a 1.5 percentage change in this criterion (Table 3). Hence, it is crucial for policymakers to pay utmost attention to the impacts that exhibit elastic burden-shifting responsiveness.

6. Results and discussion

This section applies the proposed methodology to categorize and quantify burden-shifting between life cycle impacts when different targets on GWP100 are imposed in line with the 2 °C and 1.5 °C emissions mitigation pathways.

6.1. The trade-offs between the cost of electricity and targets on global warming potential

Fig. 4 shows the Pareto frontier obtained by running ERCOM-LCIA 1,000 times (as described in Fig. 2), where each run imposes a different upper bound on GWP100 in line with the 2 °C and, more severely, the 1.5 °C emissions mitigation pathways following the epsilon-constraint method (i.e., the targets are equally spread from a lower to an upper bound), along with the resultant energy supply portfolio. The lower and upper bounds used in the epsilon-constraint method correspond to the lowest GWP100 attained by ERCOM-LCIA and the GWP100 computed when the cost of electricity is minimized without any upper bound on the GWP100, respectively.

On analyzing the resulting mixes for every upper bound on GWP100, four noticeable displacements of technologies are observed. Firstly, from 27.44 to 27.16 kg of CO_2-Eq, coal plants are mostly replaced with PV rural and biomass power plants; this is due to the competitive GWP100 performance of the latter technologies in contrast to the large GHG footprint of coal plants. Secondly, when imposing targets between 27.16 and 26.28 kg of CO_2-Eq, the model decides to replace natural gas plants with natural gas with CCS plants to meet the increasing targets on GWP100 in a cost-effective manner. Thirdly, targets within the range 26.27–25.71 kg of CO_2-Eq displace PV, geothermal and natural gas with and without CCS, mainly with wind onshore and, to a lesser extent, biomass and hydropower plants. Lastly, for meeting targets from 25.70 kg of CO_2-Eq to the minimum feasible GWP100 value in the Pareto front (i.e., 25.28 kg of CO_2-Eq) the model deploys wind offshore plants by replacing, to some extent, wind onshore, natural gas with CCS and PV plants.

Two well-differentiated regions in the Pareto set are identified, i.e., from 26.04 to 27.44 kg CO_2-Eq (or from 26.30 to 26.24 USD_{2013}), where the slope is smooth, and from 25.28 to 26.04 kg CO_2-Eq (or from 27.04 to 26.30 USD_{2013}), where the slope becomes steeper; the latter corresponds to the last 15% of the Pareto points (Fig. 4). A deeper analysis of the curve considering the electricity mixes associated with each Pareto point reveals that such sharp increase

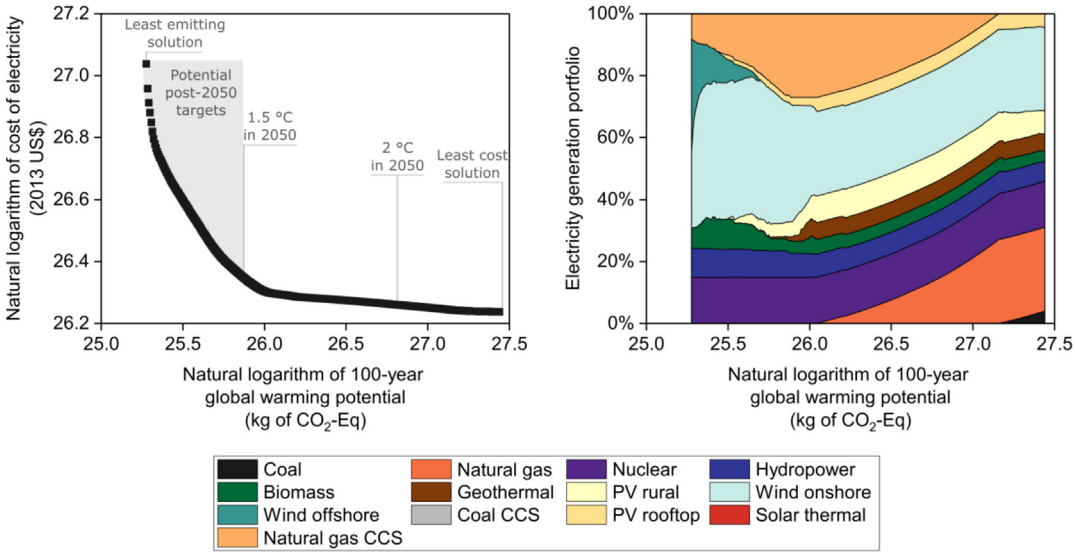

Fig. 4. Natural logarithm of the cost of electricity supply and 100-year global warming potential Pareto frontier and the resultant energy mix. Scatter plot on the left represents the natural logarithm of the least cost of electricity supply solution that meets a decreasing upper bound on the 100-year global warming potential. Area plot on the right represents the corresponding energy mix for every point on the Pareto frontier shown on the left.

in the cost of electricity supply, which takes place when stringent targets in line with the 1.5 °C emissions mitigation pathways on GWP100 are imposed, is due to the introduction of relatively expensive renewable technologies, such as wind offshore plants. Furthermore, the reliance on intermittent technologies capable of meeting the strictest targets on GWP100 forces the grid to invest in backup capacities to ensure reliability at all times, Eq. (B.13) in Appendix B, which in turn contributes further to increasing the cost of electricity supply.

6.2. Categories of burden-shifting across life cycle impacts

Fig. 5 shows the natural logarithm of selected life cycle metrics plotted against the natural logarithms of cost and GWP100. Some impacts increase with GWP100, while others decrease; this trend occasionally depends on the specific target value on the GWP100.

The graphical analysis of Fig. 5 is not straightforward, particularly when many life cycle impacts are involved. Hence, to underpin the study of burden-shifting, the Pareto points are fitted to the ICE model, Eq. (7), leading to categories and sub-categories of burden-shifting that are defined in Table 4. These sub-categories depend on the sign and magnitude of the cost and GWP100 elasticities. The sign of each elasticity determines the occurrence of burden-shifting, while its magnitude represents the severity. All in all, understanding the trend of each explanatory variable (i.e., cost of electricity and GWP100) is critical to accurately define each sub-category. Recall that, in this case, the cost of electricity increases with the last 15% of the strictest upper bounds on GWP100 as described in subsection 6.1.

Table 5 shows the calculated elasticities as a result of fitting the life cycle impacts of every Pareto point shown in Fig. 4 to the ICE model, Eq. (7). Overall, applying Eq. (7) results in good R^2 values in all the cases (Table 5). Furthermore, all the p-values of the derived fit for each life cycle impact are very close to zero, while p-values of

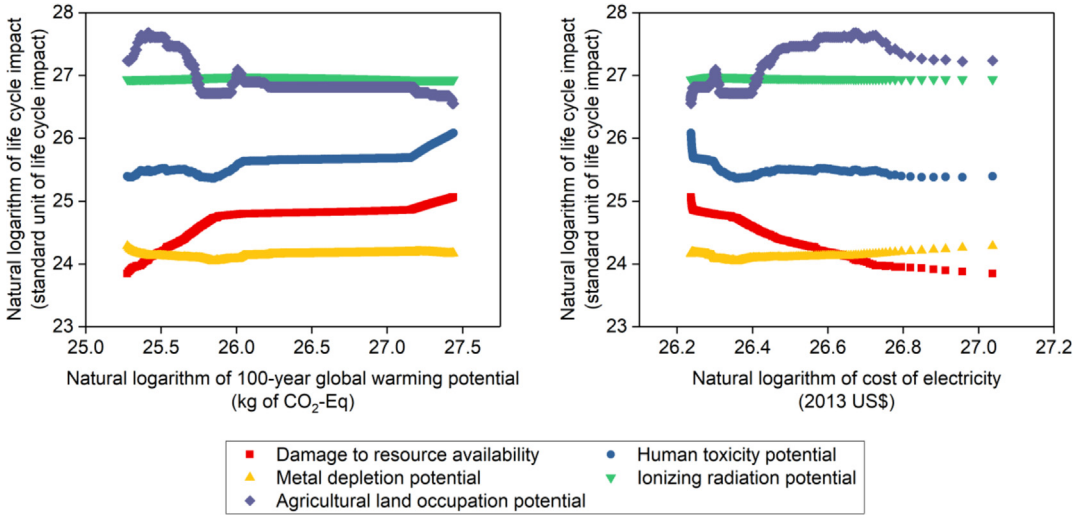
Natural logarithm of life cycle impact (standard unit of life cycle impact)
Natural logarithm of 100-year global warming potential (kg of CO2-Eq)
Natural logarithm of cost of electricity (2013 US$)
Damage to resource availability
Metal depletion potential
Agricultural land occupation potential
Human toxicity potential
Ionizing radiation potential

Fig. 5. Natural logarithm of selected life cycle impacts as a function of the natural logarithm of the 100-year global warming potential (scatter plot on the left) and the natural logarithm of the cost of electricity supply (scatter plot on the right). Standard units of life cycle impacts are shown in Table 1.

Table 4
Burden-shifting sub-categories description and signs of the cost and GWP100 elasticities. GWP100 denotes the 100-year global warming potential. The mathematical relationship between the cost and GWP100 elasticities are also shown.

Category Type	Sub-category label	Description	Sign of the cost elasticity	Comparative magnitude of elasticities	Sign of the GWP100 elasticity
No burden-shifting	A1	Impact improves with any target on GWP100	−		+
	A2	Impact improves with low to medium GWP100 targets with slight improvements with high GWP100 targets	+	<	+
Total burden-shifting	B1	Impact worsens with any GWP100 target	+		−
	B2	Impact worsens with low to medium GWP100 targets with a slight worsening with high GWP100 targets	−	>	−
Partial burden-shifting	C1	Impact worsens with high GWP100 targets only	+	>	+
	C2	Impact worsens with low to medium GWP100 targets only	−	<	−

Table 5
Cost of electricity and GWP100 elasticities and intercepts as a result of fitting every life cycle impact of every Pareto point to the ICE model, Eq. (7). GWP100 denotes the 100-year global warming potential. Ordinal R^2 and burden-shifting sub-category type are reported where the latter is described in Table 4.

Impact	Cost elasticity	GWP100 elasticity	Intercept	Ordinal R^2	Sub-category type	Impact	Cost elasticity	GWP100 elasticity	Intercept	Ordinal R^2	Sub-category type
Terrestrial ecotoxicity potential	−1.64	0.40	51.08	0.95	A1	Agricultural land occupation potential	1.41	−0.06	−8.80	0.74	B1
Damage to resource availability	−1.54	0.08	63.13	0.94	A1	Damage to ecosystem diversity	1.64	0.37	−43.90	0.74	C1
Marine ecotoxicity potential	−0.18	0.14	23.96	0.94	A1	Metal depletion potential	0.17	0.06	17.87	0.63	C1
Particulate matter formation potential	−0.25	0.09	24.17	0.65	A1	Ozone depletion potential	−1.33	−0.24	53.30	0.92	C2
Terrestrial acidification potential	−0.08	0.15	19.23	0.56	A1	Fossil depletion potential	−1.84	−0.01	74.94	0.92	C2
Damage to human health	0.28	0.74	−13.50	1.00	A2	Ionizing radiation potential	−0.17	−0.05	32.63	0.92	C2
Freshwater ecotoxicity potential	0.16	0.34	9.94	0.99	A2	Urban land occupation potential	−2.13	−0.02	79.83	0.91	C2
Marine eutrophication potential	0.56	0.64	−12.74	0.97	A2	Natural land transformation potential	−3.13	−0.70	119.33	0.90	C2
Human toxicity potential	0.27	0.28	11.22	0.73	A2	Water depletion potential	−0.92	−0.05	47.57	0.88	C2
Freshwater eutrophication potential	0.52	0.55	−10.11	0.65	A2	Photochemical oxidant formation potential	−0.60	−0.08	39.08	0.34	C2

*All the p-values of the explanatory variables and intercept of each life cycle impact are below 0.05. All the p-values of the models are very close to zero.

the explanatory variables and intercepts are below 0.05. Hence, all the derived interpretations can be assumed to be broadly valid and in line with those reported in Table 4.

Next, the considered life cycle impacts are grouped into the three categories described in Table 2: total burden-shifting, no burden-shifting and partial burden-shifting – with elasticities in the range from −3.13 to 1.64 (Table 5). While GWP100 exhibits inelastic elasticities only, cost exhibits both elastic and inelastic elasticities. Broadly speaking, a percentage change in the cost affects life cycle impacts more than a percentage change in GWP100. In other words, stringent targets on GWP100 would induce greater percentage changes in the life cycle impacts compared to low to medium targets on GWP100.

A deeper analysis on the calculated elasticities reveals two different sub-categories for each of the three burden-shifting categories highlighted in Table 2; these can be established based on the elasticities signs and their comparative magnitudes (Table 5). Before describing each sub-category, recall that in this particular problem the cost increases rapidly in the last 15% of the targets on GWP100 (Fig. 4). Therefore, the cost elasticity plays an important role, mainly within the last 15% of the more stringent GWP100 targets, whereas GWP100 elasticity plays a greater role in the first 85% of the GWP100 targets (i.e., low to medium targets). As shown in Fig. 4, stringent GWP100 targets in line with the 1.5 °C mitigation pathways increase the cost, making it the main explanatory variable. On the other hand, targets in line with the 2 °C emissions mitigation pathways do not noticeably increase the cost so the GWP100 becomes the main explanatory variable. The aforementioned insight is critical in analyzing the sub-categories, which are in general GWP100 target-dependent.

Within category A, which contains ten life cycle impacts, there is no burden-shifting at all with any target on GWP100. Overall, this category exhibits a relatively high average R^2 of around 84% while the explanatory variables and intercept levels fall within the acceptable threshold of p-values (Table 5). Further analysis of the elasticities in Category A delineates two sub-categories that differ in the sign and comparative magnitude of elasticities (Table 4). The first sub-category shows negative cost elasticities and positive GWP100 elasticities, implying that impacts belonging to this category improve with any GWP100 target. In other words, when GWP100 decreases, the corresponding impact in sub-category A1 decreases as well, and when the cost increases, the corresponding impact decreases too. The second sub-category has positive cost and GWP100 elasticities, albeit the latter elasticities are greater in magnitude than the former. Therefore, impacts belonging to sub-category A2 decrease when GWP100 decreases and do so with a lower slope when the cost increases; this occurs because the GWP100 elasticity exerts a greater force on the opposite direction than the cost elasticity, counterbalancing the effect of the latter.

Category B denotes total burden-shifting with any GWP100

target. There is only one impact in this category, with a good R^2 of 74% and p-values within the acceptable thresholds of the explanatory variables and intercept (Table 5). Although two types of sub-categories could be theoretically defined within category B, only one of them is found in practice; nevertheless, both are described for completeness (Table 4). The first sub-category shows a positive cost elasticity and a negative GWP100 elasticity. This implies that the impact belonging to sub-category B1 worsens when the GWP100 decreases and cost increases. On the other hand, sub-category B2 shows both negative cost and GWP100 elasticities, though the latter elasticity, in absolute value, is greater than the former. Therefore, an impact belonging to this sub-category would worsen when GWP100 decreases, as the GWP100 elasticity is greater, in absolute value, than the cost elasticity, thereby offsetting the latter effect.

Category C reflects partial burden-shifting (i.e., GWP100 target-dependent burden-shifting). This category encompasses nine life cycle impacts. Overall, category C shows a good average R^2 of around 80%, with p-values of the explanatory variables and intercept within the acceptable threshold (Table 5). Category C has two sub-categories that differ in the sign and comparative magnitude of elasticities (Table 4). Sub-category C1 shows positive cost and GWP100 elasticities, where the former elasticity is greater than the latter. Therefore, the impact improves when GWP100 decreases, yet it worsens when the cost increases sharply; this happens because the cost elasticity offsets the effect of the GWP100 elasticity. This sub-category can be found in the 1.5 °C emissions mitigation pathways, in which severe targets imposed on GWP100 increase the cost substantially (Fig. 4). On the other hand, sub-category C2 shows negative cost and GWP100 elasticities, where the former elasticities are greater, in absolute value, than the latter. Hence, the impact worsens when GWP100 decreases and improves when the cost increases. Again, since the cost elasticity is greater, in absolute value, than the GWP100 elasticity, the former offsets the latter; this sub-category arises in the 2 °C emissions mitigation pathways where low to medium targets are imposed on GWP100.

6.3. Category A: no burden-shifting

Here, life cycle impacts belonging to category A are described. This subsection explores in detail the differences between each life cycle impact belonging to category A in each sub-category in terms of elasticities and R^2. Overall, there are ten life cycle impacts belonging to Category A.

6.3.1. Sub-category A1

Sub-category A1 contains five life cycle impacts, namely terrestrial ecotoxicity potential, damage to resource availability, marine ecotoxicity potential, particulate matter formation potential and terrestrial acidification potential. Furthermore, this sub-category shows a good fit with an average R^2 of 81% (Table 5). Sub-category A1 shows negative cost elasticities and positive GWP100 elasticities (Table 4). As discussed in subsection 6.2, life cycle impacts belonging to sub-category A1 improve with any target on GWP100 (Fig. 6). Therefore, these impacts should be of less concern to policymakers, since electricity technologies with good performance in GWP100 would also perform well in life cycle impacts belonging to sub-category A1.

The magnitude of the elasticities provides insight into the severity of burden-shifting. Although they all follow the same trend as GWP100 and opposite trend to the cost, they differ in their elasticities and goodness of the fit. The best fits are found in terrestrial ecotoxicity potential, damage to resource availability and marine ecotoxicity potential (Table 5). Concerning the elasticities, terrestrial ecotoxicity potential and damage to resource availability are elastic with respect to the cost. This implies that these impacts exhibit greater improvements when the cost increases due to stringent targets on GWP100. This happens because both elasticities are greater than one in absolute value terms, indicating that for each percentage unit of change in the cost, while keeping other factors constant, terrestrial ecotoxicity potential and damage to resource availability will exhibit 1.64 and 1.54 percentage changes, respectively (Table 5).

6.3.2. Sub-category A2

Sub-category A2 has five life cycle impacts that include damage to human health, freshwater ecotoxicity potential, marine eutrophication potential, human toxicity potential and freshwater eutrophication potential. Overall, sub-category A2 shows a better average fit than sub-category A1, with an average R^2 of 87% (Table 5). Life cycle impacts belonging to sub-category A2 have positive cost and GWP100 elasticities, where the latter are greater than the former (Table 4). Due to the elasticities in sub-category A2, the impacts improve when GWP100 decreases, though such improvement mitigates when the cost increases (Fig. 7). Like in sub-category A1, policymakers should not worry about these life cycle impacts when attempting to curb GHG emissions.

Impacts belonging to sub-category A2 differ mainly in the goodness of their fit and magnitude of elasticities. For instance, damage to human health, freshwater ecotoxicity potential and marine eutrophication potential show the best fits in this sub-category (Table 5). Moreover, all the calculated elasticities in sub-category A2 are inelastic. Therefore, one percentage change in GWP100, when all other factors are held constant, leads to a percentage change below one in all impacts belonging to sub-category A2. This inelastic behavior is given by the magnitude of elasticities in sub-category A2, all below one. Since the cost elasticity is lower than the GWP100 elasticity, when the cost increases the impact decreases (i.e., on a net basis, the GWP100 elasticity overrules the effect of the cost elasticity).

6.4. Category B: total burden-shifting

This subsection describes the life cycle impact belonging to category B. This category is further divided into two sub-categories, albeit only one impact is found in one of the sub-categories (i.e., sub-category B1) while the other one is empty in this case study. Here, only the impact belonging to category B, i.e., agricultural land occupation potential, is described.

Category B shows total burden-shifting with any target on GWP100. The only impact in this category, agricultural land occupation potential, has a relatively good fit with an R^2 of 74%. The agricultural land occupation potential shows a positive cost elasticity and a negative GWP100 elasticity. Hence, agricultural land occupation increases when the GWP100 decreases and the cost increases (Fig. 8). This highlights the vulnerability of such impact to any target on GWP100. Therefore, policymakers need to pay attention to impacts belonging to category B, since burden-shifting could take place under any target imposed on GWP100. This occurs because electricity technologies with competitive GWP100 values tend to have poor agricultural land occupation footprint (e.g., biomass power plants).

The agricultural land occupation potential shows elastic responsiveness to the cost (Table 5). In other words, one unit of percentage change in cost, keeping other factors constant, yields 1.41 percentage change in agricultural land occupation potential (Table 5). Hence, when 1.5 °C emissions mitigation pathways are enforced (i.e., when stringent targets on GWP100 are imposed), the agricultural land occupation potential would worsen the most. On the other hand, agricultural land occupation has inelastic and very

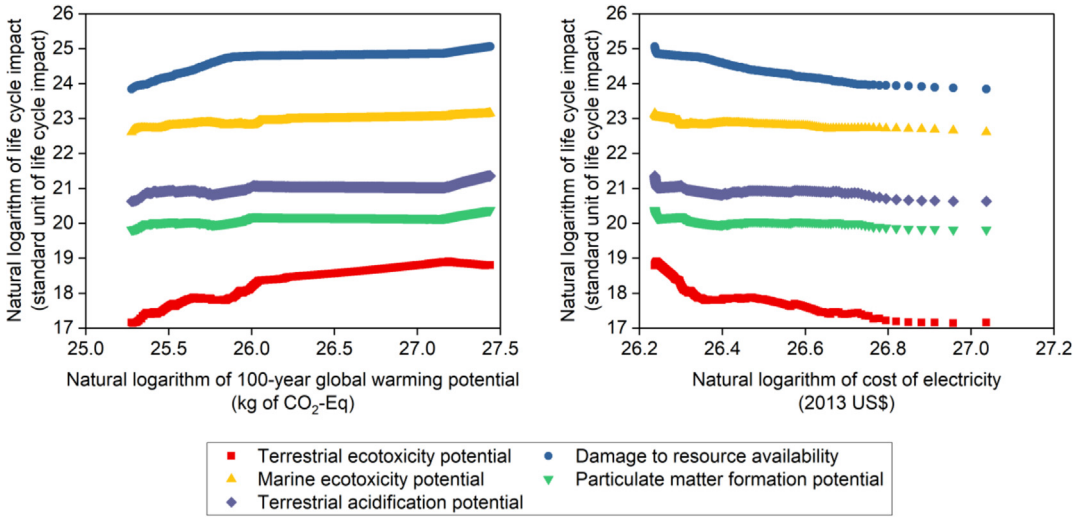
Natural logarithm of life cycle impact (standard unit of life cycle impact)
Natural logarithm of 100-year global warming potential (kg of CO_2-Eq)
Natural logarithm of cost of electricity (2013 US$)
Terrestrial ecotoxicity potential
Marine ecotoxicity potential
Terrestrial acidification potential
Damage to resource availability
Particulate matter formation potential

Fig. 6. Natural logarithm of the life cycle impacts in sub-category A1 as a function of the natural logarithm of the 100-year global warming potential (scatter plot on the left) and the natural logarithm of the cost of electricity supply (scatter plot on the right). Sub-categories are described in Table 4. Standard units of life cycle impacts are shown in Table 1.

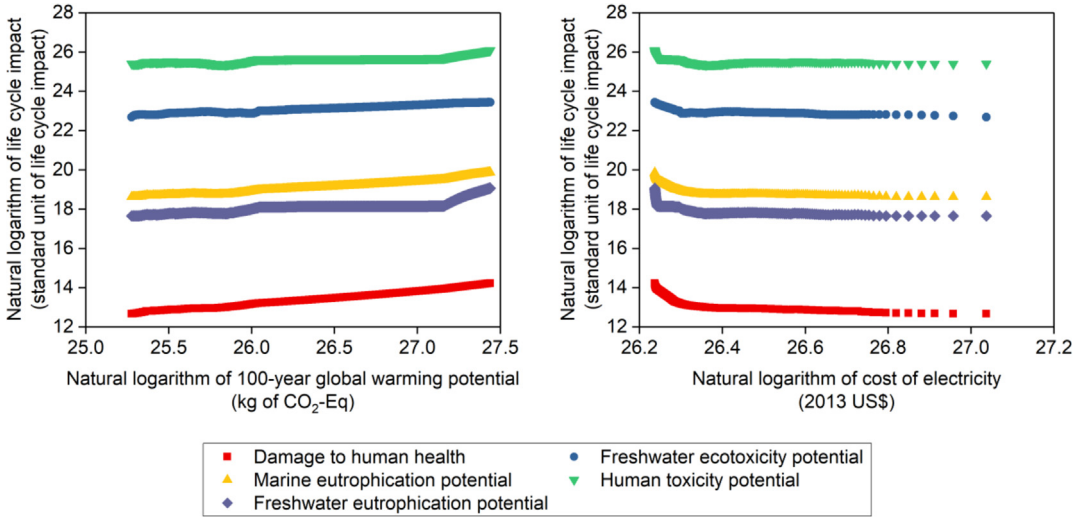
Natural logarithm of life cycle impact (standard unit of life cycle impact)
Natural logarithm of 100-year global warming potential (kg of CO_2-Eq)
Natural logarithm of cost of electricity (2013 US$)
Damage to human health
Marine eutrophication potential
Freshwater eutrophication potential
Freshwater ecotoxicity potential
Human toxicity potential

Fig. 7. Natural logarithm of the life cycle impacts in sub-category A2 as a function of the natural logarithm of the 100-year global warming potential (scatter plot on the left) and the natural logarithm of the cost of electricity supply (scatter plot on the right). Sub-categories are described in Table 4. Standard units of life cycle impacts are shown in Table 1.

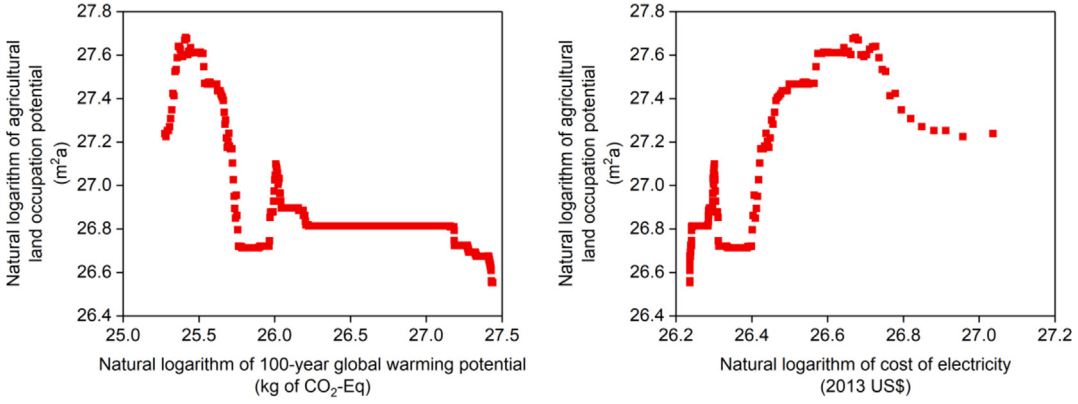
Natural logarithm of agricultural land occupation potential (m^2a)
Natural logarithm of 100-year global warming potential (kg of CO_2-Eq)
Natural logarithm of cost of electricity (2013 US$)

Fig. 8. Natural logarithm of the life cycle impact in sub-category B1 (i.e., the agricultural land occupation potential) as a function of the natural logarithm of the 100-year global warming potential (scatter plot on the left) and the natural logarithm of the cost of electricity supply (scatter plot on the right). Sub-categories are described in Table 4.

low responsiveness to GWP100 (i.e., an elasticity of −0.06), which explains the low increase in agricultural land occupation potential when low to medium targets are imposed on GWP100.

6.5. Category C: partial burden-shifting

In this subsection, the third and most challenging category of burden-shifting is described. Category C deals with partial burden-shifting; that is, burden-shifting depends on the severity of the target on GWP100. There are two sub-categories belonging to category C, explained in detail in the following subsections.

6.5.1. Sub-category C1

Two life cycle impacts are found in sub-category C1, namely damage to ecosystem diversity and metal depletion potential. Overall, impacts belonging to this sub-category show reasonable fits with an average R^2 of 69% (Table 5). They have positive cost and GWP100 elasticities, though the former elasticities are greater than the latter. Therefore, life cycle impacts in this sub-category improve with low to medium targets on GWP100 due to the positive GWP100 elasticities, yet they worsen when the cost increases due to the greater positive cost elasticities compared to the GWP100 elasticities (Fig. 9). Consequently, policymakers need to pay special attention to life cycle impacts in this sub-category when stringent targets on GWP100 are imposed.

Impacts in sub-category C1 differ in the goodness of the fit and magnitude of elasticities. The damage to ecosystem diversity impact has a slightly better fit than the metal depletion potential. The magnitude of the elasticities is also critical when determining the severity of burden-shifting. Although both ecosystem diversity and metal depletion impacts worsen when cost increases, the former exhibits an elastic response to the cost (Fig. 9). For instance, one percentage change in cost, while keeping other factors constant, yields a 1.64 percentage change in damage to ecosystem diversity and only 0.17 percentage change in metal depletion potential (Table 5).

6.5.2. Sub-category C2

There are seven life cycle impacts in sub-category C2, including ozone depletion, fossil depletion, ionizing radiation, urban land occupation, natural land transformation, water depletion and photochemical oxidant formation potentials, with an average R^2 of 83% (Table 5). Impacts belonging to sub-category C2 feature negative cost and GWP100 elasticities, though, in absolute value, the former elasticities are greater than the latter. Hence, burden-shifting occurs with low to medium targets due to the negative GWP100 elasticities; however, they improve when the cost increases due to the greater, in absolute value, negative cost elasticities compared to the GWP100 (Fig. 10). Therefore, policymakers need to pay attention to impacts belonging to sub-category C2 when low to medium targets on GWP100 are imposed in line with the 2 °C emissions mitigation pathways.

Impacts in sub-category C2 differ in the goodness of their fit and the magnitude of elasticities. For instance, all impacts in sub-category C2 except photochemical occident formation potential exhibit high R^2 (Table 5). Furthermore, natural land transformation, urban land occupation, fossil depletion and ozone depletion potentials show elastic responses to the cost; that is, one percentage change in cost, when other factors are held constant, leads to 3.13, 2.13, 1.84 and 1.33 percentage changes in these impacts, respectively (Table 5). All impacts have inelastic responses to GWP100, with the natural land transformation potential showing the highest, in absolute value, GWP100 elasticity. Therefore, natural land transformation potential would incur the highest damage across impacts in sub-category C2 when imposing low to medium targets on GWP100.

7. Conclusions

Policies of narrow scope focusing only on a subset of the full spectrum of sustainability criteria could induce trade-offs or burden-shifting across them; that is, one sustainability problem could be solved by creating another. Recent environmental policies, such as the Paris Agreement, took climate change as their main priority. Nonetheless, electricity technologies with competitive GWP100 performance might not perform that well on other sustainability criteria. Therefore, comprehensive policy frameworks whereby all sustainability criteria are evaluated and improved concurrently need to be developed to underpin ongoing global environmental discussions.

To demonstrate the limitations of environmental policies focusing only on specific environmental impacts, a statistical framework coupled with multi-objective optimization and LCA was developed, which allows identifying the occurrence and severity of burden-shifting across sustainability criteria. The developed framework was applied to the design of an energy mix considering twenty impacts quantified via the ReCiPe 2008 framework. Three categories of burden-shifting across life cycle

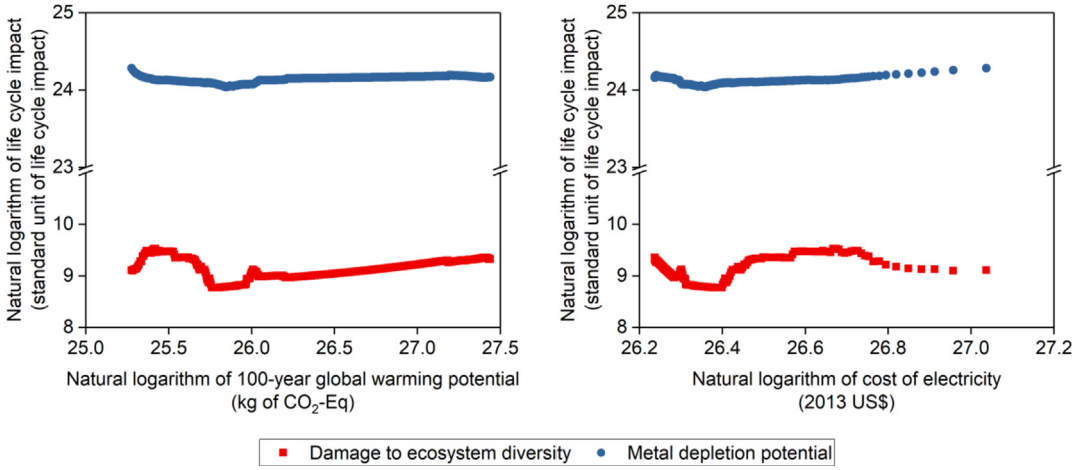

Fig. 9. Natural logarithm of the life cycle impacts in sub-category C1 as a function of the natural logarithm of the 100-year global warming potential (scatter plot on the left) and the natural logarithm of the cost of electricity supply (scatter plot on the right). Sub-categories are described in Table 4. Standard units of life cycle impacts are shown in Table 1.

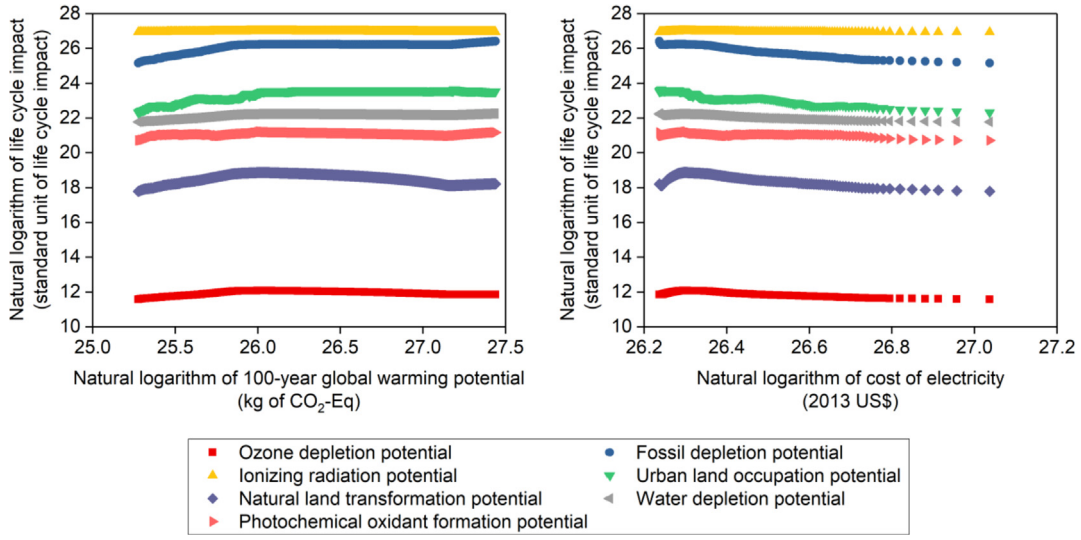
Natural logarithm of life cycle impact (standard unit of life cycle impact)
Natural logarithm of 100-year global warming potential (kg of CO_2-Eq)
Natural logarithm of cost of electricity (2013 US$)
Ozone depletion potential
Ionizing radiation potential
Natural land transformation potential
Photochemical oxidant formation potential
Fossil depletion potential
Urban land occupation potential
Water depletion potential

Fig. 10. Natural logarithm of the life cycle impacts in sub-category C2 as a function of the natural logarithm of the 100-year global warming potential (scatter plot on the left) and the natural logarithm of the cost of electricity supply (scatter plot on the right). Sub-categories are described in Table 4. Standard units of life cycle impacts are shown in Table 1.

impacts were identified when attempting to mitigate the GWP100: no burden-shifting, total burden-shifting and partial burden-shifting. These categories, together with sub-categories within them, can be defined according to the magnitude and sign of the derived elasticities. For instance, in the partial burden-shifting sub-categories, some impacts worsen only when low to medium targets on GWP100 are imposed, while others do so with more stringent limits on GWP100. In practice, policymakers should pay the utmost attention to environmental impacts belonging to the total and partial burden-shifting categories, since they can worsen substantially depending on the stringency of the targets on GWP100.

Some of the life cycle impacts belonging to the total and partial burden-shifting categories exhibit elastic responses to the cost elasticity induced by stringent targets on GWP100. Such impacts worsen the most, since one percentage change in cost, when all other factors are held constant, yields a percentage change above one in such elastic life cycle impacts. Overall, there is no energy mix capable of mitigating all life cycle impact simultaneously while reducing the GWP100. Hence, further research is needed to quantify the extent to which life cycle impacts could be worsened to ultimately improve others, with emphasis on GWP100.

Designing policies that would minimize all the environmental metrics without worsening others on the way could be increasingly complex. Therefore, defining budgets for each life cycle impact could be very insightful and useful to policymakers; that is, one impact could be improved at the expense of another, yet without exceeding a given ecological threshold (Child et al., 2018). These ecological budgets could be designed following the recent concept of planetary boundaries (Steffen et al., 2015), whereby global thresholds are established to limit certain environmental stressors that, if transgressed, could trigger harmful nonlinear changes to the Earth. Though some life cycle impacts were considered in such framework of planetary boundaries (Ryberg et al., 2018), others are still missing and warrant further research (Algunaibet et al., 2019b).

Declarations of interest

None.

Acknowledgments

Ibrahim M. Algunaibet thanks Saudi Aramco for the full PhD scholarship. Gonzalo Guillén-Gosálbez acknowledges the financial support from NERC – Natural Environment Research Council (NE/P019900/1). Gonzalo Guillén-Gosálbez thanks the Spanish Ministry of Education and Competitiveness (CTQ2016-77968-C3-1-P, MINECO/FEDER) for the received financial support. All authors thank the anonymous reviewers for their insightful comments.

Appendix A. Nomenclature

Indices

i	Electricity technologies
j	States
k	Neighboring Canadian regions
l	Life cycle impacts (midpoints and endpoints)

Sets

CT	Electricity generated via coal and coal with carbon capture and storage technologies
IR	Intermittent electricity technologies that include photovoltaics rural and rooftop, wind onshore and offshore, solar thermal and hydropower
NGT	Electricity generated via natural gas and natural gas with carbon capture and storage technologies
NC_j	Neighboring Canadian regions to state j
NU_j	Neighboring states to state j

Parameters

BUC	Reliability factor representing the ratio of backup capacity of dispatchable technologies to the capacity of intermittent technologies
$CAP_{i,j}^{CUR}$	Capacity in 2012 of electricity technology i and state j
$CF_{i,j}$	Capacity factor of electricity technology i and state j
CO^{CAN}	Price of electricity imports from neighboring Canadian regions
$CO_{i,j}^{CAP}$	Capital cost of electricity technology i and state j
$CO_{i,j}^{FIX}$	Fixed operating cost of electricity technology i and state j

$CO_{i,j}^{VAR}$ Variable operating cost of electricity technology i and state j
CTB Highest share of demand that can be met by electricity imports from neighboring Canadian regions
DEM_j Electricity demand in state j
$DIST_{j,j'}$ Distance of transmission from state j to state j'
$DISTCAN_{j,k}$ Distance of transmission from state j to neighboring Canadian region k
DSF Electricity demand satisfaction factor
$CF_{i,j,l}$ Characterization factor linked to life cycle impact l for electricity generated via technology i and state j
$GEN_{i,j}^{POT}$ Potential electricity generation by electricity technology i and state j
GEN_i^{POTGLO} Total national potential of electricity generation by electricity technology i
$GWP100_{i,j}$ 100-year global warming potential of every unit of electricity generated by technology i and state j
H Number of hours in a given year

$TARG$ Varying target on the total life cycle value of the 100-year global warming potential due to electricity supply
TLF Electricity generation Losses as a result of transmission

Continuous variables
$CAP_{i,j}^{BU}$ Backup Capacity installed of electricity technology i and state j
$CAP_{i,j}^{ST}$ Standard Capacity installed of electricity technology i and state j
$COST_j$ Electricity generation cost in state j
$COST_j^{CAN}$ Electricity imports cost from neighboring Canadian regions to state j
$COST_j^{CAP}$ Electricity generation capital cost in state j
$COST_j^{FIX}$ Electricity generation fixed operating cost in state j
$COST^{TOT}$ Cost of electricity generation in the United States
$COST_j^{VAR}$ Electricity generation variable operating cost in state j
EM_j Total value of the 100-year global warming potential due to electricity generation in state j
$GEN_{i,j}^{BU}$ Electricity generated by backup technology i and state j
$GEN_{i,j}^{ST}$ Electricity generated by standard technology i and state j
I_l Total amount of the life cycle impact l
$TRD_{j,j'}^{DEST}$ Total amount of electricity exports from state j' to neighboring state j
$TRD_{j,j'}^{LOSS}$ Electricity losses incurred during transmission due to exports from state j' to neighboring state j
$TRD_{j,j'}^{ORIG}$ Total amount of electricity exports from state j' to neighboring state j
$TRDCAN_{j,k}^{DEST}$ Exports of electricity from neighboring Canadian region k to state j
$TRDCAN_{j,k}^{LOSS}$ Electricity losses incurred during transmission due to exports from neighboring Canadian region k to state j
$TRDCAN_{j,k}^{ORIG}$ Total amount of electricity exports from neighboring Canadian region k to state j

Appendix B. The mathematical formulation of the Emissions Reduction Cooperation Model with Life Cycle Impact Assessment (ERCOM-LCIA)

$$\sum_j EM_j \le TARG \tag{B.1}$$

$$EM_j = \sum_i \left(GEN_{i,j}^{ST} GWP100_{i,j}\right) + \sum_i \left(GEN_{i,j}^{BU} GWP100_{i,j}\right) \quad \forall j \tag{B.2}$$

$$I_l = \sum_{i,j} \left(\left(GEN_{i,j}^{ST} + GEN_{i,j}^{BU}\right) CF_{i,j,l}\right) \quad \forall l \tag{B.3}$$

$$GEN_{i,j}^{ST} + GEN_{i,j}^{BU} \le GEN_{i,j}^{POT} \quad \forall j, i \neq coal, coal\ CCS, natural\ gas, natural\ gas\ CCS \tag{B.4}$$

$$\sum_{i \in CT} \left(GEN_{i,j}^{ST} + GEN_{i,j}^{BU}\right) \le GEN_{i',j}^{POT} \quad \forall j, i' = coal \tag{B.5}$$

$$\sum_{i \in NGT} \left(GEN_{i,j}^{ST} + GEN_{i,j}^{BU}\right) \le GEN_{i',j}^{POT} \quad \forall j, i' = natural\ gas \tag{B.6}$$

$$\sum_{j, i \in CT} \left(GEN_{i,j}^{ST} + GEN_{i,j}^{BU}\right) \le GEN_{i'}^{POTGLO} \quad \forall\ i' = coal \tag{B.7}$$

$$\sum_{j, i \in NGT} \left(GEN_{i,j}^{ST} + GEN_{i,j}^{BU}\right) \le GEN_{i'}^{POTGLO} \quad \forall\ i' = natural\ gas \tag{B.8}$$

$$\sum_j \left(GEN_{i,j}^{ST} + GEN_{i,j}^{BU}\right) \le GEN_i^{POTGLO} \quad \forall\ i = biomass \tag{B.9}$$

$$GEN_{i,j}^{ST} \le CAP_{i,j}^{ST} CF_{i,j} H \quad \forall i, j \tag{B.10}$$

$$GEN_{i,j}^{BU} = CAP_{i,j}^{BU} CF_{i,j} H \quad \forall i, j \tag{B.11}$$

$$CAP_{i,j}^{ST} + CAP_{i,j}^{BU} = CAP_{i,j}^{CUR} \quad \forall j, i = nuclear \tag{B.12}$$

$$\sum_{i \notin IR} CAP_{i,j}^{BU} = BUC \sum_{i \in IR} CAP_{i,j}^{ST} \quad \forall j \tag{B.13}$$

$$CAP_{i,j}^{BU} = 0 \quad \forall j, i \in IR \tag{B.14}$$

$$TRD_{j,j'}^{ORIG} = 0 \quad \forall j, j' \notin NU_j \tag{B.15}$$

$$TRDCAN_{j,k}^{ORIG} = 0 \qquad \forall j,k \notin NC_j \tag{B.16}$$

$$TRD_{j,j'}^{ORIG} = TRD_{j,j'}^{DEST} + TRD_{j,j'}^{LOSS} \qquad \forall j,j' \in NU_j \tag{B.17}$$

$$TRDCAN_{j,k}^{ORIG} = TRDCAN_{j,k}^{DEST} + TRDCAN_{j,k}^{LOSS} \qquad \forall j,k \in NC_j \tag{B.18}$$

$$TRD_{j,j'}^{LOSS} = TRD_{j,j'}^{ORIG} DIST_{j,j'} TLF \qquad \forall j,j' \in NU_j \tag{B.19}$$

$$TRDCAN_{j,k}^{LOSS} = TRDCAN_{j,k}^{ORIG} DISTCAN_{j,k} TLF \qquad \forall j,k \in NC_j \tag{B.20}$$

$$\sum_{j,k \in NC_j} TRDCAN_{j,k}^{ORIG} \leq CTB \sum_{j} DEM_j \tag{B.21}$$

$$\sum_{j' \in NU_j} TRD_{j,j'}^{DEST} + \sum_{k \in NC_j} TRDCAN_{j,k}^{DEST} \leq DEM_j \qquad \forall j \tag{B.22}$$

$$\sum_{i} GEN_{i,j}^{ST} + \sum_{i \notin IR} GEN_{i,j}^{BU} + \sum_{j' \in NU_j} TRD_{j,j'}^{DEST} + \sum_{k \in NC_j} TRDCAN_{j,k}^{DEST} - \sum_{j' \in NU_j} TRD_{j',j}^{ORIG} = DEM_j DSF \qquad \forall j \tag{B.23}$$

$$COST^{TOT} = \sum_{j} COST_j \tag{B.24}$$

$$COST_j = COST_j^{CAP} + COST_j^{FIX} + COST_j^{VAR} + COST_j^{CAN} \forall j \tag{B.25}$$

$$COST_j^{CAP} = \sum_{i} \left(\left(CAP_{i,j}^{ST} + CAP_{i,j}^{BU} \right) CO_{i,j}^{CAP} CF_{i,j} H \right) \qquad \forall j \tag{B.26}$$

$$COST_j^{FIX} = \sum_{i} \left(\left(CAP_{i,j}^{ST} + CAP_{i,j}^{BU} \right) CO_{i,j}^{FIX} CF_{i,j} H \right) \qquad \forall j \tag{B.27}$$

$$COST_j^{VAR} = \sum_{i} \left(\left(GEN_{i,j}^{ST} + GEN_{i,j}^{BU} \right) CO_{i,j}^{VAR} \right) \qquad \forall j \tag{B.28}$$

$$COST_j^{CAN} = \sum_{k \in NC_j} TRDCAN_{j,k}^{DEST} CO^{CAN} \qquad \forall j \tag{B.29}$$

References

Algunaibet, I.M., Matar, W., 2018. The responsiveness of fuel demand to gasoline price change in passenger transport: a case study of Saudi Arabia. Energy Efficiency 11 (6), 1341–1358.

Algunaibet, I.M., Pozo, C., Galán-Martín, Á., Guillén-Gosálbez, G., 2019a. Quantifying the cost of leaving the Paris Agreement via the integration of life cycle assessment, energy systems modeling and monetization. Appl. Energy 242, 588–601.

Algunaibet, I.M., Pozo, C., Galán-Martín, Á., Huijbregts, M.A.J., Mac Dowell, N., Guillén-Gosálbez, G., 2019b. Powering sustainable development within planetary boundaries. Energy Environ. Sci. https://doi.org/10.1039/C8EE03423K.

Amorim, F., Pina, A., Gerbelova, H., da Silva, P.P., Vasconcelos, J., Martins, V., 2014. Electricity decarbonisation pathways for 2050 in Portugal: a TIMES (The Integrated MARKAL-EFOM System) based approach in closed versus open systems modelling. Energy 69, 104–112.

Brooke, A., Kendrick, D., Meeraus, A., Raman, R., Rasenthal, R., 1998. A Users Guide. GAMS Development Corporation, Washington, DC.

Chertow, M.R., 2000. The IPAT equation and its variants. J. Ind. Ecol. 4 (4), 13–29.

Child, M., Koskinen, O., Linnanen, L., Breyer, C., 2018. Sustainability guardrails for energy scenarios of the global energy transition. Renew. Sustain. Energy Rev. 91, 321–334.

Choi, S.J., Choi, D.G., Friley, P., Kim, H., Park, S.Y., 2017. Quantitative analysis on the energy and environmental impact of the Korean national energy R&D roadmap a using bottom-up energy system model. Sustainability 9 (4), 538.

Corona, B., San Miguel, G., Cerrajero, E., 2014. Life cycle assessment of concentrated solar power (CSP) and the influence of hybridising with natural gas. Int. J. Life Cycle Assess. 19 (6), 1264–1275.

Ehrlich, P.R., Holdren, J.P., 1972. Critique. Bull. At. Sci. 28 (5), 16–27.

EIA, 2011. The Electricity Market Module of the National Energy Modeling System: Model Documentation. US Energy Information Administration.

Fripp, M., 2012. Switch: a planning tool for power systems with large shares of intermittent renewable energy. Environ. Sci. Technol. 46 (11), 6371–6378.

Galan-Martin, A., Pozo, C., Azapagic, A., Grossmann, I.E., Mac Dowell, N., Guillen-Gosalbez, G., 2018. Time for global action: an optimised cooperative approach towards effective climate change mitigation. Energy Environ. Sci. 11 (3), 572–581.

Garcia-Gusano, D., Garrain, D., Dufour, J., 2017. Prospective life cycle assessment of the Spanish electricity production. Renew. Sustain. Energy Rev. 75, 21–34.

García-Gusano, D., Iribarren, D., Dufour, J., 2018. Is coal extension a sensible option for energy planning? A combined energy systems modelling and life cycle assessment approach. Energy Policy 114, 413–421.

Goedkoop, M., Heijungs, R., Huijbregts, M., De Schryver, A., Struijs, J., Van Zelm, R., 2009. ReCiPe 2008. A Life Cycle Impact Assessment Method Which Comprises Harmonised Category Indicators at the Midpoint and the Endpoint Level 1.

Grossman, G.M., Krueger, A.B., 1995. Economic growth and the environment. Q. J. Econ. 110 (2), 353–377.

IEA, 2018. Electricity Information 2018: Overview. International Energy Agency.

Iribarren, D., Petrakopoulou, F., Dufour, J., 2013. Environmental and thermodynamic evaluation of CO2 capture, transport and storage with and without enhanced resource recovery. Energy 50, 477–485.

ISO, I., 2006. 14040: Environmental Management–Life Cycle Assessment–Principles and Framework. British Standards Institution, London.

Limleamthong, P., Guillen-Gosalbez, G., 2017. Rigorous analysis of Pareto fronts in sustainability studies based on bilevel optimization: application to the redesign of the UK electricity mix. J. Clean. Prod. 164, 1602–1613.

Loulou, R., Goldstein, G., Noble, K., 2004. Documentation for the MARKAL family of models. Energy Technol. Syst. Anal. Program. 65–73.

Mas-Colell, A., Whinston, M.D., Green, J.R., 1995. Microeconomic Theory. Oxford university press, New York.

McDowall, W., Rodriguez, B.S., Usubiaga, A., Fernández, J.A., 2018. Is the optimal decarbonization pathway influenced by indirect emissions? Incorporating indirect life-cycle carbon dioxide emissions into a European TIMES model. J. Clean. Prod. 170, 260–268.

Mendoza, J.M.F., Popa, S.A., D'Aponte, F., Gualtieri, D., Azapagic, A., 2019. Improving resource efficiency and environmental impacts through novel design and manufacturing of disposable baby diapers. J. Clean. Prod. 210, 916–928.

Murillo-Alvarado, P.E., Guillén-Gosálbez, G., Ponce-Ortega, J.M., Castro-Montoya, A.J., Serna-González, M., Jiménez, L., 2015. Multi-objective optimization of the supply chain of biofuels from residues of the tequila industry in Mexico. J. Clean. Prod. 108, 422–441.

Organization, I.S., 1997. ISO 14040: Environmental Management-Life Cycle Assessment-Principles and Framework.

Pehl, M., Arvesen, A., Humpenoder, F., Popp, A., Hertwich, E.G., Luderer, G., 2017. Understanding future emissions from low-carbon power systems by integration of life-cycle assessment and integrated energy modelling. Nature Energy 2 (12), 939–945.

Petrakopoulou, F., Iribarren, D., Dufour, J., 2015. Life-cycle performance of natural gas power plants with pre-combustion CO2 capture. Greenhouse Gases: Sci. Technol. 5 (3), 268–276.

Rauner, S., Budzinski, M., 2017. Holistic energy system modeling combining multi-objective optimization and life cycle assessment. Environ. Res. Lett. 12 (12), 124005.

Reinhard, J., Zah, R., 2009. Global environmental consequences of increased biodiesel consumption in Switzerland: consequential life cycle assessment. J. Clean. Prod. 17, S46–S56.

Ryberg, M.W., Owsianiak, M., Richardson, K., Hauschild, M.Z., 2018. Development of a life-cycle impact assessment methodology linked to the Planetary Boundaries framework. Ecol. Indicat. 88, 250–262.

Statistics, U.S.B.o.L., 2018. Consumer Price Index, Consumer Price Index. U.S. Department of Labor, United States.

Steffen, W., Richardson, K., Rockstrom, J., Cornell, S.E., Fetzer, I., Bennett, E.M., Biggs, R., Carpenter, S.R., de Vries, W., de Wit, C.A., Folke, C., Gerten, D., Heinke, J., Mace, G.M., Persson, L.M., Ramanathan, V., Reyers, B., Sorlin, S., 2015. Sustainability. Planetary boundaries: guiding human development on a changing planet. Science 347 (6223), 1259855.

Suman, S., 2018. Hybrid nuclear-renewable energy systems: a review. J. Clean. Prod. 181, 166–177.

UNFCCC, 2015a. Adoption of the Paris Agreement. UNFCCC, Bonn, Germany.

UNFCCC, 2015b. United States Intended Nationally Determined Contribution under the Paris Agreement. United Nations Framework Convention on Climate

Change.
Wernet, G., Bauer, C., Steubing, B., Reinhard, J., Moreno-Ruiz, E., Weidema, B., 2016. The ecoinvent database version 3 (part I): overview and methodology. Int. J. Life Cycle Assess. 21 (9), 1218–1230.
York, R., Rosa, E.A., Dietz, T., 2003. STIRPAT, IPAT and ImPACT: analytic tools for unpacking the driving forces of environmental impacts. Ecol. Econ. 46 (3), 351–365.